Materials Science and Engineering B 172 (2010) 187–190

Contents lists available at ScienceDirect

Materials Science and Engineering B

journal homepage: www.elsevier.com/locate/mseb

Enhance of electrical properties of resistive switches based on $Sr_{0.1}Ba_{0.9}TiO_3$ and TiO_2 thin films by employing a Ni–Cr alloy as contact

E. Hernández-Rodríguez [a,*], A. Márquez-Herrera [a], M. Meléndez-Lira [b], M. Zapata-Torres [a]

[a] Centro de Investigación en Ciencia Aplicada y Tecnología Avanzada del IPN, Legaria #694 Col. Irrigación C.P., 11500 México D.F., Mexico
[b] Departamento de Física, CINVESTAV-IPN, Apartado Postal 14-740, 07000 México D.F., Mexico

ARTICLE INFO

Article history:
Received 17 March 2010
Received in revised form 13 May 2010
Accepted 19 May 2010

Keywords:
Oxides
Metal–insulator–metal structures
Electrical measurements
Sputtering

ABSTRACT

We have investigated the electric-field-induced resistance-switching phenomena of ReRAM cells based on $Sr_{0.1}Ba_{0.9}TiO_3$ and TiO_2 thin films fabricated by rf-sputtering technique. Thin films were sandwiched between Pt, Ti and nichrome bottom electrode and Cu top electrode. The *I–V* measurements at room temperature are non-linear and hysteretic. Cells based on $Sr_{0.1}Ba_{0.9}TiO_3$ present a unipolar resistance-switching phenomenon and it is symmetric with respect to the voltage polarity, while cells based on TiO_2 have a bipolar resistance-switching with asymmetric behavior. From the *I–V* measurements we demonstrated that the nichrome enhances the resistance-switching characteristics of the cells. A reduction of the voltage needed to achieve the HRS–LRS and LRS–HRS transitions are found and a very clear transition between these states is accomplished, in comparison with ReRAM cells fabricated with Pt and Ti electrodes, whose voltage values are large and no clear transitions are presented. This improvement in resistance-switching behavior can be explained due to O_2 vacancies formed in the interface because higher affinity for oxygen of nickel and chromium.

© 2010 Elsevier B.V. All rights reserved.

Electric-field-induced switching of resistance is very promising for potential applications in future high-performance non-volatile memory, known as resistance random access memory (ReRAM) [1,2]. ReRAM has several advantages, such as low-power consumption, high operation speed, long retention time, and especially due to its three-dimensional multistack structure [3]. This resistance-switching behavior has been reported in various materials, such as metal oxides [4–9] and transition metal perovskites [10,11]. Many models were proposed such as the modification of the Schottky barrier height by trapped charge carriers [12], formation of a conductive filamentary path [13], electrical-field-induced migration of oxygen vacancies [14], carriers tunneling between crystalline defects [15], etc. However, much research is still required, from which the reversible transition mechanisms can be investigated deeply and the memory performance can be optimized. In attempt to optimize resistive switching, in this work we proposed the nichrome as suitable electrode because it fulfills the requirements for construction of ReRAM memories, such as thermal stability [16] and good adhesion provided by chromium [17], and in contrast to Pt, Al, Cu, Ag and Au electrodes, nichrome has low price. ReRAM cells were prepared with $Sr_{0.1}Ba_{0.9}TiO_3$ (BST) and TiO_2 thin films using nichrome as the bottom electrode and Cu as the top electrode and their resistive switching were compared with cells using Pt and Ti as bottom electrodes prepared using the same method and under same deposition conditions.

$Sr_{0.1}Ba_{0.9}TiO_3$ and TiO_2 thin films were fabricated by rf-magnetron sputtering in an Ar/O_2 plasma. The distance between the substrate holder and the target was 80 mm and the base pressure was 5×10^{-6} Torr or less. Deposition was carried out in an off-axis configuration and sputtering was performed at a pressure of 30 mTorr. Also the substrate was rotated at 100 rpm to promote a surface uniformity. TiO_2 thin films were deposited by reactive rf-sputtering from a Ti metal target at 150 W rf target power and the substrate was heated up at 345 °C. On the other hand, BST thin films were deposited by rf co-sputtering from a $BaTiO_3$ (BTO) and $SrTiO_3$ (STO) targets; A 105 and 15 W rf target powers was used, respectively. The substrate was heated to 600 °C to obtain crystalline films. In the preparation both TiO_2 and BST thin films, the mass flow of the gases introduced to the deposition chamber was kept at 15 and 5 sccm for the Ar and O_2 respectively. The deposition time was fixed at 120 min in order to obtain a film thickness about of 360 nm on TiO_2 and BST samples. To form the bottom electrode of the heterostructures, the BST and TiO_2 films were deposited on nichrome substrates obtained from a nicromel-80 0.127 mm thick commercial strip of the H. Cross company. Also, films were deposited on Pt and Ti bottom electrodes prepared on Si substrates by rf-sputtering technique from a Pt and Ti metal targets in an argon plasma. Deposition was carried out at 30 W rf target power and the deposition time was fixed at 15 min to obtain a film thickness of about 45 nm; Cu top electrode with diameter of 1 mm patterned with a metal mask was

* Corresponding author. Tel.: +52 555 7296000.
E-mail address: noehmx@hotmail.com (E. Hernández-Rodríguez).

0921-5107/$ – see front matter © 2010 Elsevier B.V. All rights reserved.
doi:10.1016/j.mseb.2010.05.017

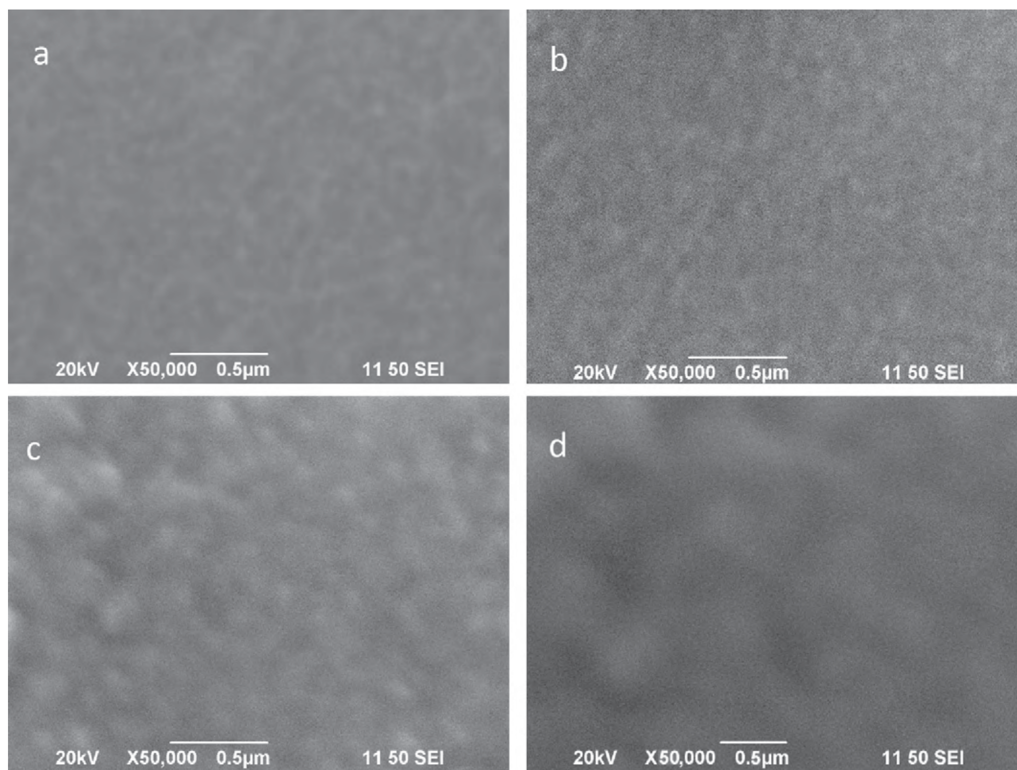

Fig. 1. Top-view SEM images of TiO_2 formed on (a) Ti and (c) nichrome and BST formed on (b) Pt and (d) nichrome.

formed by thermal evaporation. A distance of 50 mm between the source evaporation and the substrate holder was used; the deposition time was fixed at 2 min and a film thickness of 1 μm was obtained. Scanning electron microscopy (SEM) was employed to characterize the morphology of as-grown films. In order to ensure that the oxide used in the construction of the heterostructures is the expected, structural characterization was performed by X-ray diffraction technique (XRD) using a Philips X'pert spectrometer with the Cu Kα line ($\lambda_{k\alpha 1}$ = 1.54056 Å and $\lambda_{k\alpha 2}$ = 1.54439 Å). This characterization was carried out on the films already deposited on the bottom electrode of the cells. In total $Cu/Sr_{0.1}Ba_{0.9}TiO_3/Pt$, $Cu/TiO_2/Ti$, $Cu/Sr_{0.1}Ba_{0.9}TiO_3$/nichrome and Cu/TiO_2/nichrome heterostructures were prepared.

Fig. 1 displays the top-view SEM images of the TiO_2 and BST formed by rf-magnetron sputtering on Ti and nichrome, and Pt and nichrome electrodes, respectively. The microstructure of the layers is polycrystalline, consisting of grains which are slightly larger when films are deposited on nichrome. The surfaces are smooth, dense and without pores. Fig. 2 shows the results of XRD characterization both of the BST and the TiO_2 thin films. Only the spectra for the Cu/BST/nichrome and Cu/TiO_2/nichrome heterostructures are showed, nevertheless, similar results were found for the other structure containing BST and TiO_2 thin films. As can be seen in Fig. 2a, the diffraction pattern of BST film are depicted as well as the positions of the diffraction peaks corresponding to BTO taken from the 050626 card of Powder Diffraction File database (PDF); They are indicated by dotted lines. As can see, the diffraction peaks of the film (indicated by blue arrows) are shifted to slightly larger angles with respect to the position of the peaks corresponding to the BTO. In order to determinate the *x* value in the compound; we used the Vegard law [18]. We obtained the value of 0.1 for *x*, then we had $Sr_{0.1}Ba_{0.9}TiO_3$ compound in the film. On the other hand, Fig. 2b shows the diffraction pattern of the TiO_2 film, which proves that this film is composed by stoichiometric TiO_2 in anatase phase, shown the reflections in the (1 0 1) plane characteristics of this phase and that was indexed from the PDF 211272 card. Additionally, the presence of nichrome is also seen in the diffractograms.

To study the characteristics of the resistive switching behavior in heterostructures, the typical *I–V* curves were recorded with a Keithley 2410 source meter unit; a current compliance of 1 mA was used and during the electrical measurements, the bias voltage was applied to the top electrode while the bottom electrode was grounded; also, measurements were made at room temperature. Obtained curves are shown in Figs. 3 and 4. After deposition, all devices were in the high resistance state (HRS). Then, by sweeping the voltage from zero to a certain value (the set voltage), an abrupt jump of current appeared and the resistance of the device switched to the low resistance state (LRS). When sweeping again, the current suddenly dropped at a specific voltage (the reset voltage) which was always lower than the set voltage, and the resistance switched to the HRS again. *I–V* curves show that heterostructures containing the $Sr_{0.1}Ba_{0.9}TiO_3$ thin film exhibits a unipolar resistive switching behavior as can be seen in Fig. 3 and heterostructures containing the TiO_2 thin film exhibits a bipolar resistive switching behavior as can be seen in Fig. 4. Nevertheless, enhanced of resistive switching behavior of the devices are observed by using nichrome as bottom electrode. As can be seen in Fig. 3, the unipolar resistive switching for $Sr_{0.1}Ba_{0.9}TiO_3$ film was tested in two cycles, the first to switch from the HRS to the LRS and the second to perform the opposite process. In the first cycle, the bias was swept from 0 to positive voltages to the top Cu electrode. The electrical current is very low at the order of nanoamperes. When a bias voltage exceeded 13.6 V for the $Cu/Sr_{0.1}Ba_{0.9}TiO_3/Pt$ structure, the current jumped up and reached the current compliance. Then, the device exhibited a small resistance (LRS). In the second cycle, as the bias is increased the current also increases but when a value of 2.2 V is reached, the device switches from the LRS to the HRS. Nevertheless, the *I–V* curve for the $Cu/Sr_{0.1}Ba_{0.9}TiO_3$/nichrome shows that the set and reset voltages are reduced by using the nichrome instead of Pt, these values are 4.0 and 0.4 V, respectively.

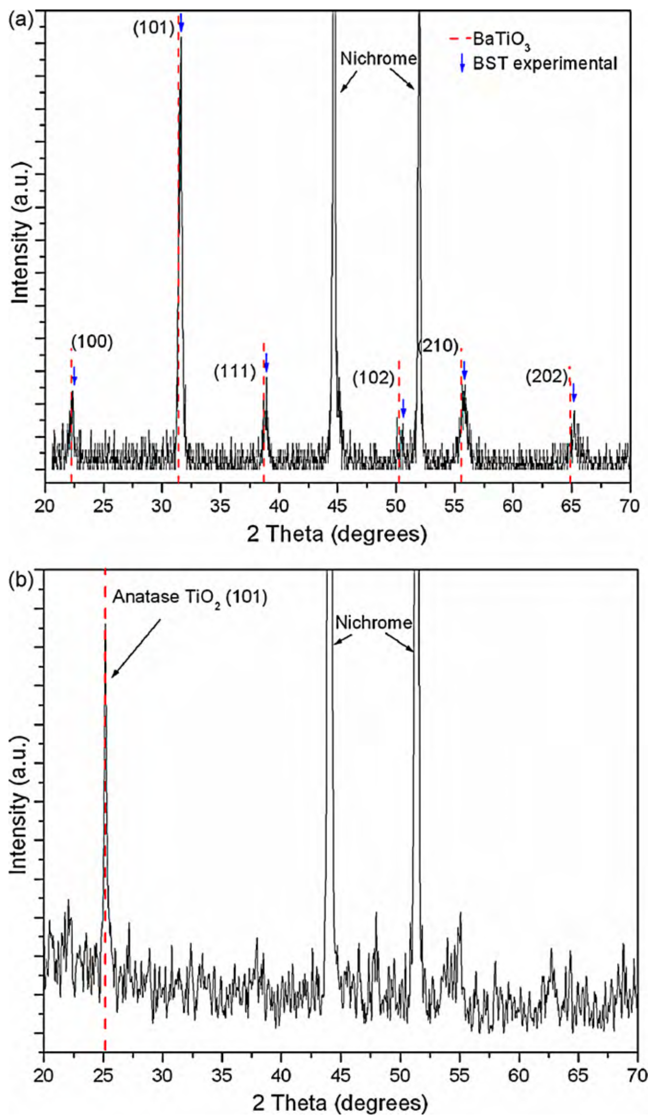

Fig. 2. X-ray diffraction patters of (a) BST and (b) TiO_2 films deposited on nichrome electrodes. The positions of the peaks show that the desired compounds are formed in the heterostructures.

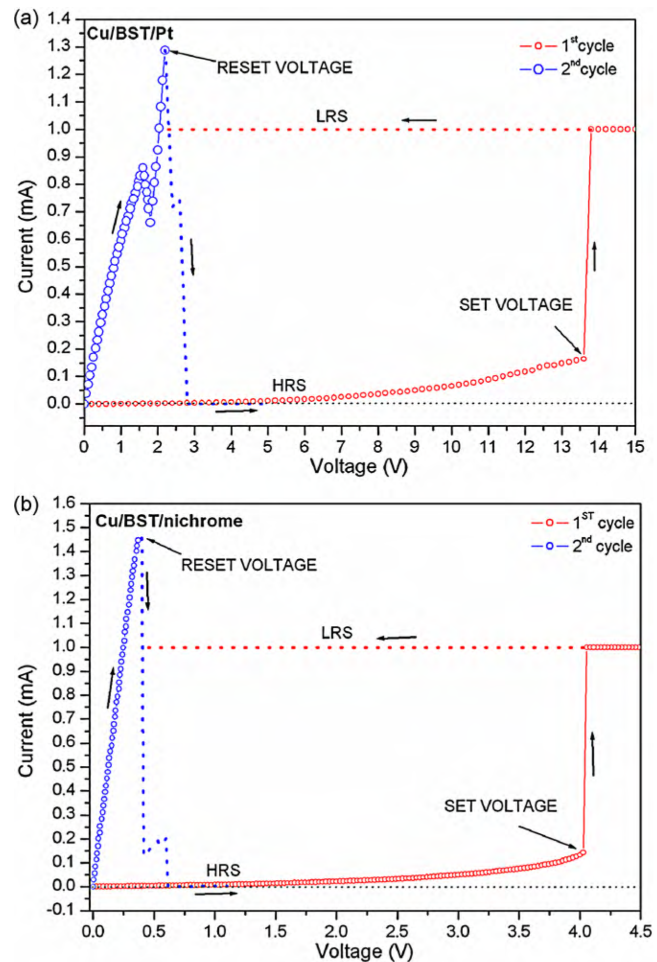

Fig. 3. Typical *I–V* curves of Cu/$Sr_{0.1}Ba_{0.9}TiO_3$/Pt (a) and Cu/$Sr_{0.1}Ba_{0.9}TiO_3$/nichrome (b) heterostructures with compliance current of 1 mA.

Fig. 4 shows the *I–V* curves of the Cu/TiO_2/Ti and Cu/TiO_2/nichrome heterostructures. Hysteresis and asymmetry phenomena were clearly observed. From Fig. 3 it can be seen that positive voltages switch the resistance to lower values (LRS) and negative voltages switch to higher values (HRS). Also, it is worth noting that this bipolar switching behavior is different from the unipolar behavior showed by the heterostructures containing $Sr_{0.1}Ba_{0.9}TiO_3$ thin films. Here, one can note that a forming process is necessary to initialize the switching property. Nevertheless, Fig. 4a in comparison with Fig. 4b shows that an enhancement in resistive switching is achieved by using nichrome as bottom electrode. Under a voltage sweep, it is evident that the set and reset voltages are very large for the device with Ti bottom electrode and the forming process requires high voltages, however, the nichrome bottom electrode drastically reduces the voltages above mentioned, also, the hysteresis curve shows a very clear transitions between the HRS and the LRS. A 1.3 and −0.9 V are required to the set and reset process in contrast with those required in device with Ti bottom electrode (18.2 and −10.1 V, respectively).

Schottky contact height was determined according to the thermionic emission model by using the Cheung's functions [19,20] from *I–V* experimental data at room temperature. The obtained values were: 1.4 and 0.84 eV for the BST-Pt and BST–nichrome contacts, respectively; and 0.18 and 0.9 eV for the TiO_2–Ti and TiO_2–nichrome contacts, respectively. Therefore, the Schottky barrier must be related to the resistive switching. However, resistance-switching phenomena cannot be explained only by the Schottky contact. In perovskite oxide material (as is the BST) has been reported that the oxygen vacancies formed in the metal–semiconductor interface plays a crucial role in the resistance-switching phenomenon [14] and this probably explains the cause for improvement in resistive switching when nicromel is used as electrode in Cu/BST/nichrome heterostructure compared to Cu/BST/Pt. Since the platinum due to its nonoxidizing property does not compete for the oxygen with the BST film, oxygen vacancies are not formed in the interface, unlike the nickel and chromium, whose affinity for oxygen is higher, resulting in oxygen vacancy in the BST film, which therefore may be the cause of the improvement of resistive switching properties. This presence of O_2 vacancies in resistive switches which present *I–V* hysteresis curves has been reported by Jeong et al. which provides a microscopic analysis by using HRTEM, analytical TEM and XPS techniques [21]; Liu et al. have also conducted a study on the effect of vacancies through Auger spectroscopy [22]. On the other hand, for n-type semiconductors, as the TiO_2, has been reported that, as the work function of the metal electrode increases, the contact resistance between the semiconductor and the metal electrode also increases, and this can result in a best resistive switching behavior [1]. This can probably explain

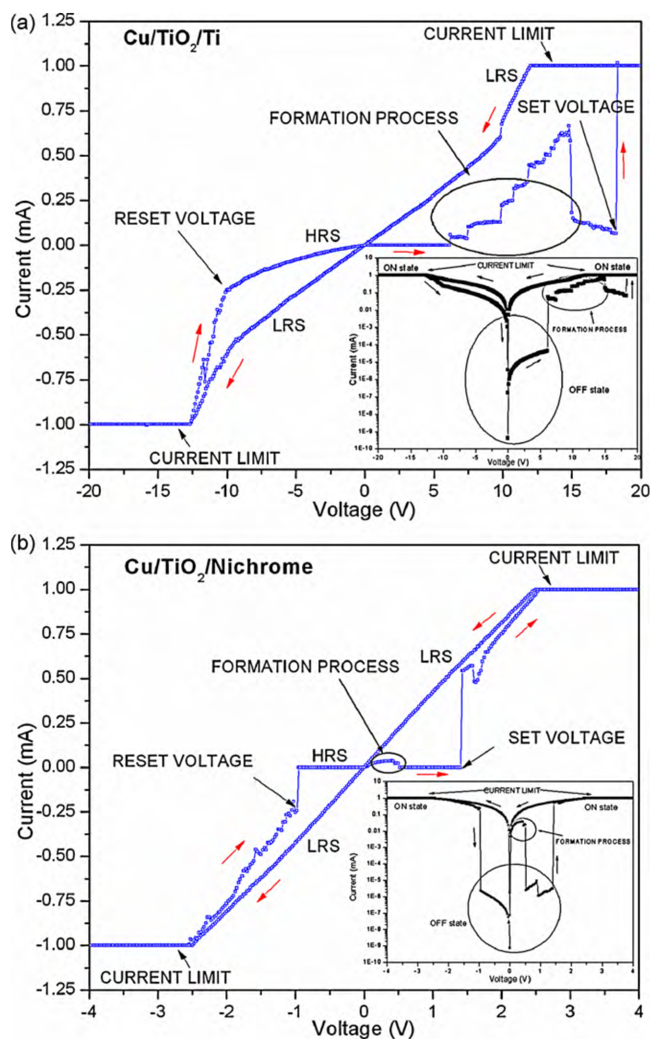

Fig. 4. Typical *I–V* curves of $Cu/TiO_2/Ti$ (a) and Cu/TiO_2/nichrome (b) heterostructures with compliance current of 1 mA. Insets on these figures show the current plotted in a logarithmic scale as function of voltage.

why the use of nichrome in the Cu/TiO_2/nichrome heterostructure improves the resistive switching compared with titanium in the $Cu/TiO_2/Ti$, because the Schottky barrier of TiO_2–nichrome is greater than TiO_2–Ti.

In summary, we studied resistive switching of heterostructures based on $Sr_{0.1}Ba_{0.9}TiO_3$ and TiO_2 thin films and investigated the effect of using *nichrome* as bottom electrode in comparison with the Pt and Ti. We showed the existence of hysteretic curves for all devices prepared in this work, and superior advantages were showed by using nichrome.

Acknowledgments

This work is supported by SEP-CONACYT and Secretaria de Investigación y Posgrado (SIP) of IPN (No. 20100117).

References

[1] Akihito, Mater. Today 11 (2008) 6–28.
[2] S.W. Wełnic, M. Wuttig, Mater. Today 11 (2008) 6–20.
[3] C. Kügeler, M. Meier, R. Rosezin, S. Gilles, R. Waser, Solid-State Electronics 53 (2009) 1287.
[4] W.-Y. Yang, W.-G. Kim, S.-W. Rhee, Thin Solid Films 517 (2008) 967.
[5] C.-Y. Lin, D.-Y. Lee, S.-Y. Wang, C.-C. Lin, T.-Y. Tseng, Surf. Coat. Technol. 203 (2008) 628.
[6] C.-Y. Lin, C.-Y. Wu, C.-Y. Wu, C.-C. Lin, T.-Y. Tseng, Thin Solid Films 516 (2007) 444.
[7] X. Cao, X.M. Li, X.D. Gao, Y.W. Zhang, X.J. Liu, Q. Wang, L.D. Chen, Appl. Phys. A 97 (2009) 883.
[8] X. Cao, X. Li, W. Yu, X. Liu, X. He, Mater. Sci. Eng. B 157 (2009) 36.
[9] M. Villafuerte, G. Juárez, S.P. de Heluani, D. Comedi, Phys. B 398 (2007) 321.
[10] N. Menou, M. Popovici, S. Clima, K. Opsomer, W. Polspoel, B. Kaczer, G. Rampelberg, K. Tomida, M.A. Pawlak, C. Detavernier, D. Pierreux, J. Swerts, J.W. Maes, D. Manger, M. Badylevich, V. Afanasiev, T. Conard, P. Favia, H. Bender, B. Brijs, W. Vandervorst, S. Van Elshocht, G. Pourtois, D.J. Wouters, S. Biesemans, J.A. Kittl, J. Appl. Phys. 106 (2009) 094101.
[11] C. Jorel, C. Vallée, P. Gonon, E. Gourvest, C. Dubarry, E. Defay, Appl. Phys. Lett. 94 (2009) 253502.
[12] T. Oka, N. Nagaosa, Appl. Phys. Lett. 85 (2005) 266403.
[13] B.J. Choi, D.S. Jeong, S.K. Kim, C. Rohde, S. Choi, J.H. Oh, H.J. Kim, C.S. Hwang, K. Szot, R. Waser, B. Reichenberg, S. Tiedke, J. Appl. Phys. 98 (2005) 033715.
[14] S.H. Jeon, B.H. Park, J. Lee, B. Lee, S. Han, Appl. Phys. Lett. 89 (2006) 042904.
[15] M.J. Rozenberg, I.H. Inoue, M.J. Sánchez, Appl. Phys. Lett. 88 (2006) 0033510.
[16] M.A. Angadi, R. Whiting, Mater. Sci. Eng. B7 (1990) L1–L4.
[17] A.E. Gershinskii, G.V. Timofeeva, N.A. Shalygina, Thin Solid Films 162 (1988) 171.
[18] L. Vegard, Z. Phys. 5 (1921) 17.
[19] S. Gholami, H. Hajghassem, M. Khajeh, IEICE Electronic Express 6 (2009) 1325.
[20] S.K. Cheung, N.W. Cheung, Appl. Phys. Lett. 49 (1986) 85.
[21] H.Y. Jeong, J.Y. Lee, S.-Y. Choi, J.W. Kim, Appl. Phys. Lett. 95 (2009) 162108.
[22] X.J. Liu, X.M. Li, Q. Wang, W.D. Yu, R. Yang, X. Cao, X.D. Gao, L.D. Chen, Solid Satate Communications 150 (2010) 137.